Variable-Temperature MFM/EFM Study of $(La_{1-x}Pr_x)_{0.67}Ca_{0.33}MnO_3$ Thin Films

S. H. Chung, S. R. Shinde, S. B. Ogale, A. Biswas, T. Venkatesan, R. L. Greene, M. Dreyer, J. B. Dottellis, A. Millis, and R. D. Gomez, *Member, IEEE*

***Abstract*—Both ferromagnetic (FM) and charge-ordered domain structures of $(La_{1-x}Pr_x)_{0.67}Ca_{0.33}MnO_3$ thin film were detected by magnetic force microscopy (MFM) and electric force microscopy (EFM) operated at low temperatures near the peak resistance temperature (T_p). The in-plane-like FM domains of submicrometer size emerge below T_p, and their magnetic interaction with an MFM tip becomes stronger as the temperature is reduced. Charge-ordered insulating regions have the strong electrostatic interaction with an EFM tip near T_p, and the interaction correlates well with the temperature dependence of resistivity of the film.**

***Index Terms*—Charge ordering, colossal magnetoresistance, EFM, low temperature, magnetic domain, MFM.**

I. Introduction

FERROMAGNETIC (FM) perovskite manganite thin films are of recent interest due to their colossal magnetoresistive property. In addition, they have tendency to phase separation into ferromagnetic–metallic and charge-ordered-insulating domains at low temperatures. A recent tunneling electron microscopy study [1] revealed that the prototypical $(La,Pr)_{5/8}Ca_{3/8}MnO_3$ system is electronically phase-separated into a submicrometer-scale mixture of the two phases and that the macroscopic magnetoresistance can be explained by percolative transport through the FM domains. Therefore, microscopic research on their electromagnetic characteristics, especially near the transition temperature, is very important for the understanding of the macroscopic properties of the perovskite manganite systems.

Atomic force microscopy (AFM) is a very powerful tool for surface studies. However, due to the difficulties of the implementation of a low-temperature AFM, limited results have been reported on manganite thin films below T_c [2]–[4]. In this work, we show that both FM and charge-ordered domain structures can be detected by magnetic force microscopy (MFM) and electric force microscopy (EFM) operated at low temperatures. We also investigated the microscopic properties of the thin films using image analysis techniques and correlated the result with the macroscopic film characteristics such as the magnetization and resistivity near the phase transition temperature.

Manuscript received February 14, 2002; revised May 22, 2002. This work was supported by UCMP NSF-MRSEC and National Science Foundation Career Award ECS-9984797.

S. H. Chung is with the Department of Physics and also with the Laboratory for Physical Sciences, University of Maryland, College Park, MD 20742 USA (e-mail: chungsh@glue.umd.edu).

S. R. Shinde, S. B. Ogale, A. Biswas, T. Venkatesan, and R. L. Greene are with the Department of Physics, University of Maryland, College Park, MD 20742 USA.

M. Dreyer and R. D. Gomez are with the Department of Electrical and Computer Engineering and also with the Laboratory for Physical Sciences, University of Maryland, College Park, MD 20742 USA (e-mail: rdgomez@eng.umd.edu).

J. B. Dottellis is with the Laboratory for Physical Sciences, College Park, MD 20740 USA.

A. Millis is with the Department of Physics, Columbia University, New York, NY 10027 USA.

Digital Object Identifier 10.1109/TMAG.2002.803165.

II. Experimental Technique

The samples are thin films of $(La_{1-x}Pr_x)_{0.67}Ca_{0.33}MnO_3$(Pr-doped LCMO) on (100) $LaAlO_3$ (LAO) or a (100) $SrTiO_3$ (STO) substrate with $x = 0.3$ and 0.4 prepared using pulsed laser deposition. The substrate temperature, laser fluence, and oxygen pressure during deposition was 820 °C, 2 J/cm^2, and 400 mtorr, respectively. The laser pulse repetition rate was 10 Hz and the films of thickness 1200– 3000 Å were deposited. After deposition, the films were cooled down to room temperature at a rate of 10 °C/min in 400 torr oxygen. The film resistivity was measured by the conventional four-point probe method and the magnetization was obtained by a superconducting quantum interference device magnetometer. The lattice parameters were measured using an X-ray diffractometer.

Our variable-temperature MFM/EFM system has been described previously [5]. It is a commercial AFM called MultiMode (by Digital Instruments, Inc., Santa Barbara, CA) modified to cool samples down to around 100 K under high vacuum condition. The temperature of the samples can be set up to 350 K with 0.2-K accuracy. The microscope measures electric or magnetic force gradients, while the tip follows the topographic contour at a distance of 50–100 nm from the sample surface (Interleave Mode). Homemade Co-coated tips were used for the MFM experiment, and tips with thin Au (or PtIr) film coatings were used for the EFM. For the EFM measurements, in addition to the standard MFM mode, a voltage is applied to the Au-coated film while the film is grounded. Thus, an electric field gradient due to electrostatic force was detected. The images were obtained without an external magnetic field.

III. Results and Discussion

The topography and the corresponding MFM images of a 3000-Å-thick Pr-doped LCMO film ($x = 0.3$) on an STO substrate are shown in Fig. 1. The grain size is about 100 nm, and the RMS roughness is 3.47 nm [Fig. 1(a)]. The resistivity measurement indicates that the insulator–metal transition occurs at a temperature $T_p = 225$ K, which is similar to the Curie temperature (T_c) as obtained by magnetization measurement. The MFM

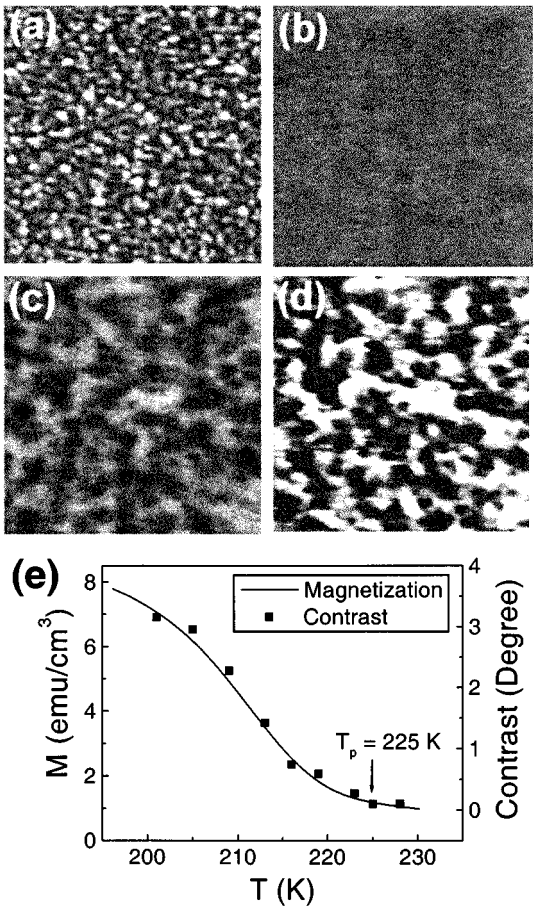

Fig. 1. Low-temperature AFM/MFM images of the Pr-doped LCMO film ($x = 0.3$) on the STO substrate. (a) Film topography. (b)–(d) Corresponding magnetic structures of the same region. These are $4 \times 4\ \mu m^2$ images at (b) 228 K, (c) 219 K, and (d) 213 K, respectively. The z scales with a maximum phase shift of 5° are the same for all of the MFM images. (e) Temperature dependence of magnetization M and the average contrast in magnetic images. The magnetization curve saturates to about 8.5 emu/cm^3 at lower temperatures. T_p is the peak resistance temperature of the sample.

images recorded at 228 K (above T_p), 219 K, and 213 K (below T_p) are shown in Fig. 1(b)–(d). Above T_p, no contrast was observed in MFM images. However, with decreasing temperature below T_p, magnetic features emerged, and the contrasts became stronger. This contrast is plotted and compared with the magnetization data measured at $H = 10$ Oe in Fig. 1(e). The contrast was obtained from the standard deviation of the histogram of the MFM images. Note the good correspondence of the independent measurements. Since MFM measures the magnetic force gradient, which is proportional to the amount and strength of magnetic charges, the contrast information of the microscopic images has the same trend as the macroscopic magnetization measurement. Similar behavior was observed for the films on LAO substrates.

Fig. 2 shows low-temperature AFM/MFM images of a 1200-Å-thick Pr-doped LCMO film ($x = 0.4$) on an LAO substrate. The grain sizes are about 90 nm, and RMS roughness is 1.40 nm. The lower RMS roughness for the films on LAO than those on STO could be due to the different nature and magnitude of the strains. LAO imposes a compressive strain (lattice mismatch $\sim -1.7\%$), whereas STO causes tensile strain

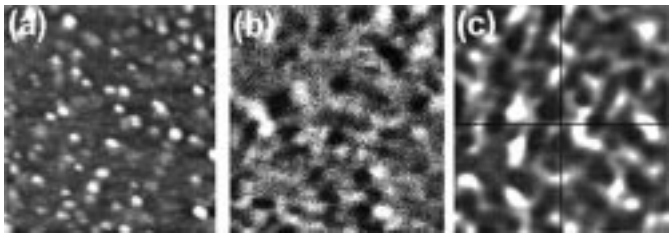

Fig. 2. Low-temperature AFM/MFM images of the Pr-doped LCMO film ($x = 0.4$) on the LAO substrate. (a) Topography of the sample surface. (b) Corresponding magnetic structure. These are $2 \times 2\ \mu m^2$ images at 153 K. (c) 2-D cross-correlation function of the images (a) and (b). The axes for displacements in the x and y directions are drawn as a guide.

in the film (lattice mismatch $\sim +1.2\%$) [6], [8]. Fig. 2(b) shows the magnetic structures as bright and dark contrasts at a temperature below $T_p = 187$ K. We note that not only the single contrasts but also dark-bright contrast pairs occur in the MFM image. Since MFM measures force gradient $\partial F(x, y)/\partial z$, those contrast pairs suggest in-plane magnetization with domains of $\sim$ 150 nm width and $\sim$ 300 nm length. This picture corresponds well to the schematic illustration of the surface structure suggested in [1]. Comparing the magnetic features for the film on LAO with those for the film on STO, one observes that the magnetic structures for the STO case are larger, more irregular, and do not occur in dark–bright pairs. This difference is probably due to the spin-canting and out-of-plane orientation of the spins resulting from the strained growth [7]. We also observed the merging and splitting of domains at temperatures near T_p, presumably because of weak interactions between magnetic domains.

A two-dimensional (2-D) cross-correlation between the topography and magnetic structure is shown in Fig. 2(c). The 2-D correlation function provides useful information of scanned images such as pattern size and distance between patterns. The position of bright regions represents the relative displacements where the topography and the MFM images are highly correlated. Note that the first maximum correlation peak is shifted from the origin by the order of the grain size. It suggests that magnetic units are likely to be found on flat regions of the surface rather than on the grain regions of the sample surface.

Fig. 3 shows the low-temperature ($T = 145$ K) EFM images of the same sample as in Fig. 2. The dark and bright contrast in Fig. 3(b) areas hundreds of nanometers in size are due to the relatively strong electrostatic interaction between the tip and the sample. The contrast became stronger with increasing voltage. However, we could not increase the voltage for better contrast because the cross talk with the topography also increases by capacitive coupling between tip and sample. The contrast vanishes at $V = \sim -0.3$ V, which probably corresponds to the contact potential difference between tip and sample materials. The EFM signal was relatively weak ($\sim$ 5 times) compared to the MFM signal. The important feature of these data is that changing the tip polarity reverses the contrast in some regions as shown in Fig. 3(b) and (c). This is highly suggestive of the presence of charge defects that occur as a consequence of electrostatic phase separation. In a detailed study of $(La,Pr)_{5/8}Ca_{3/8}MnO_3$ polycrystals in [1], the existence of charge defects and the accommodation of difference in carrier concentration by charge de-

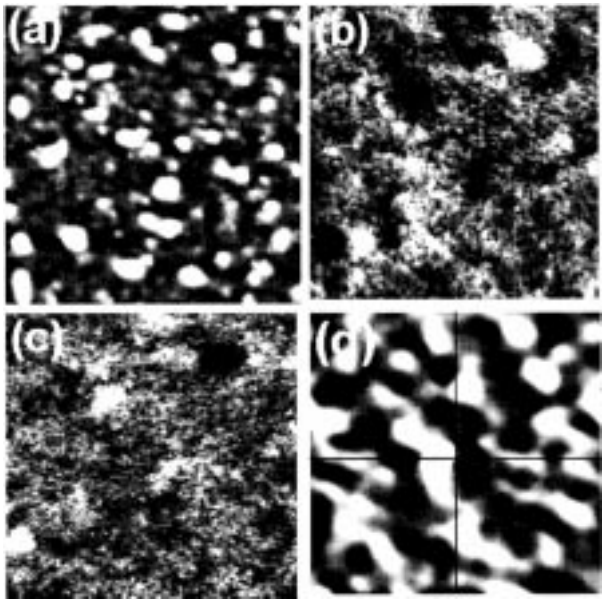

Fig. 3. Low-temperature AFM/EFM images of the Pr-doped LCMO film ($x = 0.4$) on the LAO substrate. (a) Topography of the sample. (b), (c) Corresponding electric structure with V = +0.5 and V = −0.8, respectively. They are $2 \times 2\ \mu m^2$ images at 145 K. (d) 2-D cross-correlation function of (a) and (b).

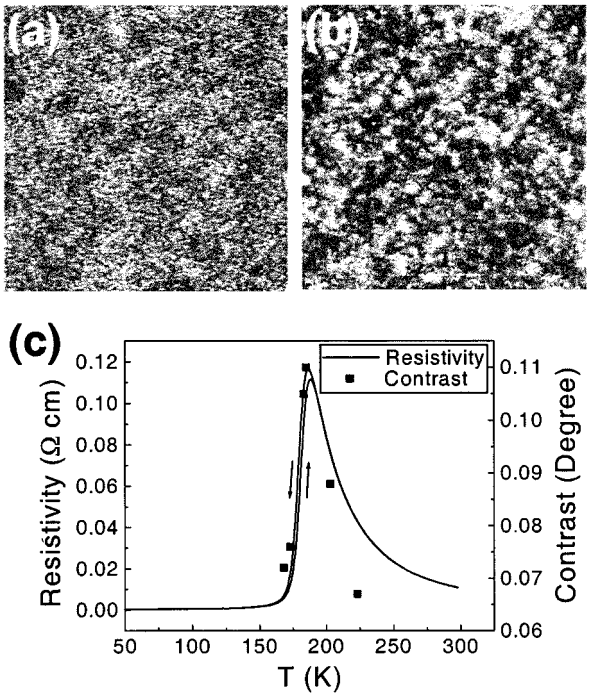

Fig. 4. Low-temperature EFM images of the Pr-doped LCMO film ($x = 0.4$) on the LAO substrate. (a), (b) $4 \times 4\ \mu m^2$ images of the electric structure of the same region. (a) At room temperature. (b) At 185 K. (c) Temperature dependence of resistivity and the average contrast in EFM images.

fects were predicted in the case of an electronically inhomogeneous system. Strong electrostatic interaction occurs near grain regions, since the first maximum of the cross-correlation function in Fig. 3(d) appears near the origin.

It should be noted that the strongest contrast in the EFM images appears near $T_p = 187$ K. As an example, EFM images at room temperature and 185 K are shown in Fig. 4(a) and (b), respectively. No contrast is observed at room temperature. However, dark and bright regions 200 nm in size are observed at 185 K. As the temperature is further reduced below T_p, the average contrast in the EFM images also decreases. The average contrast roughly follows the resistivity–temperature curve and has maximum near T_p [Fig. 4(c)]. It suggests that the temperature dependence of the resistivity could be due to a change of the characteristics of the microscopic charge-ordered phase or electric shielding effect by the FM metallic phase.

IV. Conclusion

We demonstrated that both FM and charge-ordered domain structures of thin manganite films could be detected by a low-temperature MFM/EFM system. The microscopic data near the phase transition temperature correspond well with the macroscopic film characters such as magentization and resistivity.

Acknowledgment

The authors would like to thank R. Frizzell for useful discussions and assistance.

References

[1] M. Uehara, S. Mori, C. H. Chen, and S.-W. Cheong, "Percolative phase separation underlies colossal magnetoresistance in mixed-valent manganites," *Nature*, vol. 399, pp. 560–563, 1999.

[2] Q. Lu, C.-C. Chen, and A. de Lozanne, "Observation of magnetic domain behavior in colossal magnetoresistive materials with a magnetic force microscope," *Science*, vol. 276, pp. 2006–2008, 1997.

[3] H. Oshima, Y. Ishihara, M. Nakamura, and K. Miyano, "Diffuse phase transition and magnetic-domain microstructures in a Cr-doped manganite film," *Phys. Rev. B*, vol. 63, p. 094 420, 2001.

[4] M. Fäth, S. Freisem, A. A. Menovsky, Y. Tomioka, J. Aarts, and J. A. Mydosh, "Spatially inhomogeneous metal-insulator transition in doped manganites," *Science*, vol. 285, pp. 1540–1542, 1999.

[5] S. H. Chung, S. R. Shinde, S. B. Ogale, T. Venkatesan, R. L. Greene, M. Dreyer, and R. D. Gomez, "Low temperature behavior of magnetic domains observed using a magnetic force microscope," *J. Appl. Phys.*, vol. 89, pp. 6784–6786, 2001.

[6] C. Kwon, S. E. Lofland, S. M. Bhagat, M. Rajeswari, T. Venkatesan, R. Ramesh, A. R. Krats, and R. D. Gomez, "Stress-induced surface magnetization of $(La_{0.7}Sr_{0.3})MnO_3$ thin films," *IEEE Trans. Magn.*, vol. 33, pp. 3964–3966, 1997.

[7] A. Biswas, M. Rajeswari, R. C. Srivastava, T. Venkatesan, R. L. Greene, Q. Lu, A. L. de Lozanne, and A. J. Millis, "Strain-driven charge-ordered state in $La_{0.67}Ca_{0.33}MnO_3$," *Phys. Rev. B*, vol. 63, p. 184 424, 2001.

[8] C. J. Lu, Z. L. Wang, C. Kwon, and Q. X. Jia, "Microstructure of epitaxial $La_{0.7}Ca_{0.3}MnO_3$ thin films grown on $LaAlO_3$ and $SrTiO_3$," *J. Appl. Phys.*, vol. 88, pp. 4032–4043, 2000.